Journal of Medicinal Chemistry

Brief Article

pubs.acs.org/jmc

Highly Potent HCV NS4B Inhibitors with Activity against Multiple Genotypes

Barton Phillips,* Ruby Cai, William Delaney, Zhimin Du, Mingzhe Ji, Haolun Jin, Johnny Lee, Jiayao Li, Anita Niedziela-Majka, Michael Mish, Hyung-Jung Pyun, Joe Saugier,† Neeraj Tirunagari, Jianhong Wang, Huiling Yang, Qiaoyin Wu, Chris Sheng,‡ and Catalin Zonte

Gilead Sciences, 333 Lakeside Drive, Foster City, California 94404, United States

Supporting Information

ABSTRACT: The exploration of novel inhibitors of the HCV NS4B protein that are based on a 2-oxadiazoloquinoline scaffold is described. Optimization to incorporate activity across genotypes led to a potent new series with broad activity, of which inhibitor **1** displayed the following EC_{50} values: **1a**, 0.08 nM; **1b**, 0.10 nM; **2a**, 3 nM; **2b**, 0.6 nM, **3a**, 3.7 nM; **4a**, 0.9 nM; **6a**, 3.1 nM.

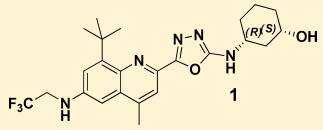

1

INTRODUCTION

Infection with the hepatitis C virus (HCV) is a global health concern, with more than 170 million affected people worldwide, including 4 million in the U.S.[1] HCV is a diverse disease, with six major HCV genotypes (GTs 1−6) and 52 sub-GTs (1a, 1b, 2a, 2b, 3a, etc.). In North America and Europe, HCV GTs 1a and 1b are most prevalent, but over 25% of patients are infected with GTs 2 and 3.[2] In North Africa and the Middle East, GT 4 is prevalent, while GT 6 predominates in East Asia.[3] Because of the lack of the proofreading ability in the HCV RNA dependent RNA polymerase,[4] high genetic variability and polymorphism occur, even within the subgenotypes. Because of the high variability in the virus, developing direct acting antivirals effective across all genotypes is challenging. The recently approved protease inhibitors (telaprevir and boceprevir) are highly effective against GT 1 but lack pan-genotype activity. Furthermore, viral strains resistant to protease inhibitors have emerged, demonstrating the need for other direct-acting antiviral agents with complementary mechanisms of action.[5] A multidrug combination regimen, without interferon and effective across HCV GTs, remains a major goal of antiviral research.

Most current clinical compounds and approved drugs targeting HCV act at and induce mutations in one of three targets: the NS3, NS5A, and NS5B proteins.[6] NS4B, or HCV nonstructural 4B, is a more recent target for HCV inhibitors. NS4B is a 27 kDa integral membrane protein believed to act primarily as an endoplasmic reticulum-localized scaffold for the assembly of the replicase complexes needed for HCV RNA replication.[7] Recently, several chemotypes that target NS4B and inhibit HCV GT 1 replication have been reported, including clemizole **1**, imidazopyridines (e.g., anguizole **2**),[8−10] 6-(indol-2-yl)pyridine-3-sulfonamides (e.g., PTC-725 **3**)[11,12] (Figure 1), and piperazinones.[13] Although highly potent GT 1 inhibitors have emerged, particularly in the imidazopyridine series, to date no agents with potent GT 2 activity have been described.[9] An analysis of the 19 available GT 2a sequences in the HCV European database revealed that the NS4B proteins of all of these strains have the variants T, L, and L at positions 94, 98, and 105, respectively, suggesting that these differences contribute to the reduced activity of NS4B inhibitors against 2a strains. In this paper we describe attempts to develop a new series of NS4B inhibitors with potent activity across genotypes, focusing on GT 2a optimization.

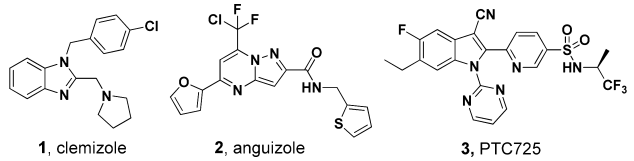

1, clemizole 2, anguizole 3, PTC725

Figure 1. Representative NS4B inhibitors.

In the course of our HCV research program we discovered a new 6,6-heterocyclic based system that provided potent inhibitors of the NS4B replicon. Compound **4** (Figure 2) is a representative early lead from this series, showing potent inhibition against the wild-type GT 1a and 1b replicons, with EC_{50}'s of 0.9 and 1.3 nM, respectively. A 42-fold shift in potency against the GT 1b-H94N replicon was observed, a polymorph well-known to be less sensitive to other small molecule NS4B inhibitors.[9,11] Furthermore, **4** showed high

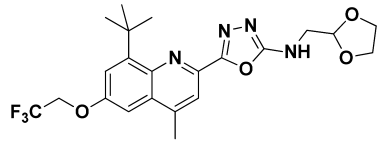

4

EC_{50} -1a = 0.9 nM
EC_{50}-1b = 1.3 nM
EC_{50}-1bH94N = 54 nM
EC_{50}-2a = 3578 nM
Pred Cl = 0.09 L/hKg

Figure 2. Early quinolone scaffold inhibitor.

Special Issue: HCV Therapies

Received: October 23, 2013
Published: February 10, 2014

binding affinity for the NS4B protein; titration with purified wild type GT 1b NS4B protein afforded a K_d of 31 nM. The GT 2a replicon also proved to be much less sensitive to compounds from the series, with a dramatic (2725-fold) drop in activity for **4**. Potent activity in GT 2a was needed for the targeted broad genotype inhibitor profile, and thus, activity at GT 2a became a major focus of optimization efforts.

CHEMISTRY

The synthesis of **4** (Scheme 1) is representative of all the compounds in the series. Beginning with 4-amino-3-*tert*-butylphenol **5**, protection of the phenol as its benzyl ether was followed by a two-step, one-pot condensation with diethyl acetylenedicarboxylate and subsequent cyclization under thermal conditions, providing quinolone **6**, which served as a versatile intermediate.

Scheme 1. Synthesis of Oxadiazole 4[a]

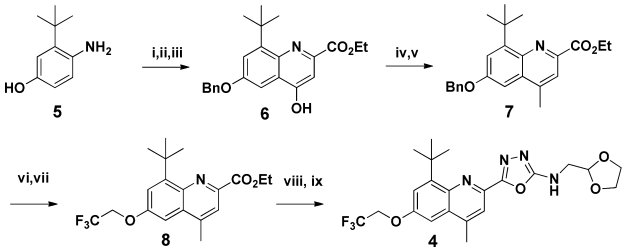

[a]Conditions: (i) BnBr, NaH, DMSO, 64%; (ii) diethylacetylene dicarboxylate, EtOH, 60 °C, 1 h; (iii) neat, 220 °C, 15 min, 73%; (iv) Tf_2O, lutidine, 0 °C, 1 h, 96%; (v) $MeB(OH)_2$, Pd(dppf)-CH_2Cl_2, Cs_2CO_3, dioxane, 100 °C, 4 h, 100%; (vi) H_2, Pd−C, 1 h, 92%; (vii) 2,2,2-trifluoroethyl trifluoromethanesulfonate, K_2CO_3, DMF, 100 °C, 4 h, 51%; (viii) hydrazine hydrate, EtOH, 70 °C, 1 h, 100%; (ix) *O*-phenyl (1,3-dioxolan-2-yl)methylcarbamothioate, TEA, EDCI (3.5 equiv), DMF 16 h, 74%.

The C-4 Me functionality was conveniently installed via Suzuki coupling of the intermediate triflate derivative with methylboronic acid. To introduce the C-6 2,2,2-trifluoroethyl ether functionality, debenzylation was followed by alkylation of the phenol to provide **8**. The 2-aminooxadiazole was generated at the end of the synthesis via a two-step procedure beginning with formation of the acyl hydrazide and followed by condensation with the appropriate phenyl thiocarbamate in the presence of EDCI to selectively remove H_2S.

RESULTS AND DISCUSSION

Compound **9** (Table 1), the initial hit in the series, showed promising activity against GT 1b but was clearly limited by high lipophilicity and low potency against GT 2a. Efforts at optimization focused on (1) reducing log *D* to 3.5 or below and (2) improving potency in GT 2a into the low nanomolar range, both combining to provide a target LLE of 4.5. New analogues were screened for inhibition of the HCV GT 1a, 1b, 1b-H94N, and 2-JFH replicon assays. LLEs were calculated from measured log *D* and GT 2a activity. Given the exceptionally low potency seen in the 2a-JFH replicon, it served as a surrogate for untested genotypes during the preliminary assessment. Table 1 outlines representative SAR from these efforts, along with predicted clearance values derived from stability upon incubation with human liver microsomes (HLMs).

Early efforts focused on modifying the flat, hydrophobic phenyl groups at each end of the inhibitor. Alkyl ethers, such as methylene-1,3-dioxolane, proved to be equipotent with phenyl as the aminooxadiazole substituent, while O-linked alkyl ethers were effective replacements for the C6 phenyl. Combining both changes in **10** gave similar activity to **9** in GT 1b but little improvement in GT 2a activity. The greatly reduced log *D* of **10**, however, resulted in a substantial increase in LLE. In contrast, smaller alkyl substituents at C6, such as **11**, provided a sharp drop in potency. Replacing the C6 ether O with the corresponding N-linker (e.g., aniline **12**) produced a drop in lipophilicity with an improvement in potency. This combination proved critical in optimizing the final compounds.

The *tert*-butyl group at C8 in **4** provided a 4-fold increase in potency over the corresponding trifluoromethyl analogue **10**, in GTs 1b and 2a. The increase in potency was sufficient to improve LLE despite a small increase in log *D*. Less lipophilic side chains such as trifluoromethyl were consistently less active, and the drop in log *D* was insufficient to offset this.

A variety of unsubstituted alkyl substituents on the aminooxadiazole, such as cyclopentyl **14**, proved to be similar in activity to the dioxolane. Unfortunately, the increase in log *D* for the unsubstituted alkyls led to a sharp drop in LLE and was typically accompanied by an increase in the rate of metabolism, a common but not universal trend in the higher log *D* analogues prepared. Adding hydroxyl substituents to the cycloalkyl proved to be very effective in reducing metabolism, and in some isomers it increased potency as well. Stereochemistry was critical for such potency increases with a 1,3-cis-substitution pattern favored for ring sizes 4−6, as illustrated in the aminocyclobutanol isomers **15** and **16**. Other substitution patterns saw no such improvement, although the trans-isomers were as stable as the corresponding cis-isomers. Given the effectiveness of the hydroxy substituents, we combined this modification with the C6 trifluoroethylanilino group. Example **18** showed an EC_{50} against 2a-JFH of 25 nM, a >10000-fold improvement over **9**, and a LLE of 3.9. In contrast, the more lipohilic ether counterpart **17** was >10-fold less active. Combined with an alcohol substituent in **18**, the C6 aniline functionality offered no liability in microsomal stability compared with C6 ether **17**. A systematic exploration of cycloalkyl alcohols revealed the (1*S*,3*R*)-*cis*-aminocyclohexanol side chain as a superior side chain, with analogue **20** showing inhibition of the GT 2a replicon in the low single digit nanomolar range, an overall increase in LLE from −0.8 to 4.9 (**9**−**20**). The cyclohexanol system was quite stereospecific, with the (1*R*,3*S*)-enantiomer of **20** being 67-fold less potent as an inhibitor in the 2a replicon system (201 nM). A resistance selection was performed with **20** using a GT 2a replicon and yielded mutations in NS4B including K20R, H53Y, L64F, and I109V.

Given the excellent potency of **20**, it was tested in a panel of replicons along with **18** and **19** to assess potency across a broad range of genotypes (Table 2). **20** displayed potent (EC_{50} < 5 nM) activity against all the replicons in this study, including GT 1b resistant polymorphs (a GT 5 replicon was not tested). Although the GT 1b vs 2a shift remained significant for **20** (30-fold), the shift was greatly reduced from that observed for **4** (2725-fold). The corresponding C6 ether **19** was much less active against GTs 2a and 3a, although it did show better stability in microsomes. Both **18** and **19** also showed a larger shift between GT 1b and GT 2a (312-fold and 300-fold, respectively). All three compounds show potential in a

dx.doi.org/10.1021/jm401646w | J. Med. Chem. 2014, 57, 2161−2166

Table 1. Inhibition of HCV RNA in the Replicon System and in Vitro Metabolic Stability

		LogD	GT 1b EC_{50} (nM) WT	GT 1b EC_{50} (nM) H94N	GT 2a – JFH(nM)	CC_{50} (nM)	LLE 2a	HLM Pred CL (L/h/kg)
9	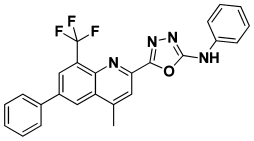	5.6	5.9	-	>20,000	86,357	< -0.8	0.46
10	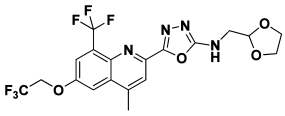	3.6	5.0	206	15,650	26,587	1.2	0.17
11	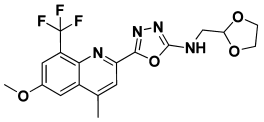	3.4	32	719	nd	50,000	nd	1.0
4	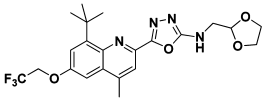	3.9	1.3	54	3578	20,423	1.6	0.09
12	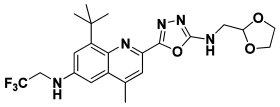	3.6	0.15	4.3	1104	16,000	2.4	0.44
13	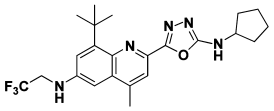	4.6	0.15	5.2	525	15,784	1.7	0.72
14	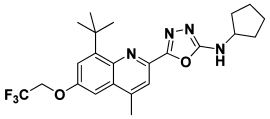	4.9	0.63	35	3033	-	0.6	0.73
15	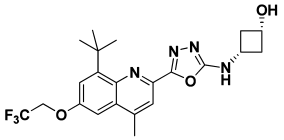	3.4	1.3	41	208	10,800	3.2	0.15
16	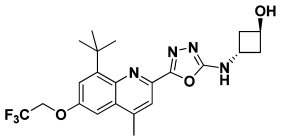	nd	3.5	714	5216	25,900	nd	0.12
17	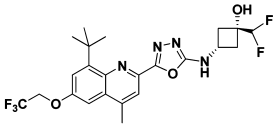	4.1	0.32	3.4	684	6,242	2.1	0.25
18	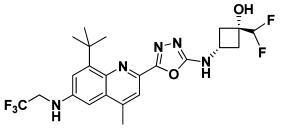	3.7	0.08	0.74	25	5,435	3.9	0.20
19	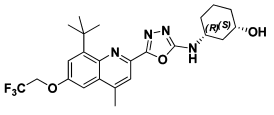	4.0	0.32	5.5	96	20,900	4.0	0.08
20	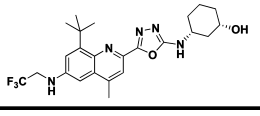	3.6	0.09	1.2	3	6,251	4.9	0.22

dx.doi.org/10.1021/jm401646w | J. Med. Chem. 2014, 57, 2161−2166

Table 2. Genotype Profile of 18, 19, and 20[a]

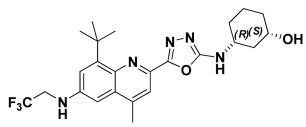

20

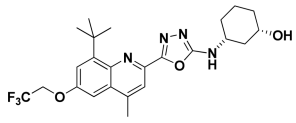

19

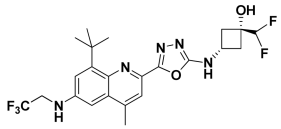

18

Replicon	EC_{50} (nM)	EC_{50} (nM)	EC_{50} (nM)
WT 1a	0.08	0.09	0.05
WT 1b	0.10	0.32	0.08
1b-H94S	0.34	-	4.4
1b-H94N	0.6	5.5	0.74
2a - JFH	3	96	25
2b	0.6	0.9	0.16
3a	3.7	30	2.3
4a	0.9	1.5	0.76
6a	3.1	-	-

[a]The GT 1a, 1b, 2a, 3a, 4a, 6a replicons are subgenomic replicons derived from only the indicated strain of HCV. The GT 2b replicon is chimeric, expressing full length GT 2b NS4B protein in backbone of a GT 2a replicon.

multigenotype drug regimen for treating HCV, with **20** holding a clear advantage due to its flatter activity profile.

DMPK. Encouraged by the results outlined above, we profiled three compounds from Table 1 in rat PK experiments. The results are summarized in Table 3, along with in vitro

Table 3. Rat pK Profile for 9, 18, and 20

compd	CL (L h^{-1} kg^{-1})	V_{ss} (L/kg)	$T_{1/2}$ (h)	F_{po} (%)	HLM (L h^{-1} kg^{-1})	RLM (L h^{-1} kg^{-1})
18	0.87	5.0	5.2	25	0.20	0.22
20	0.65	2.4	11	88	0.22	0.24
9	1.05	1.8	2.3		0.46	0.70

stability in human and rat liver microsomes (HLMs and RLMs, respectively). Compounds **18** and **20** each showed good bioavailability and relatively low CL. The high volumes help to provide a long half-life. The observed CL was slightly higher than predicted by rat liver microsomes. The initial lead **9** showed similar but somewhat inferior results, demonstrating that optimization for broader-GT potency had not compromised the in vivo PK profile of the series.

SUMMARY

We described the development of a novel series of NS4B inhibitors with broad genotype activity, starting from a lead largely limited to activity against GT 1. Early lead compounds showed an excellent pharmacokinetic profile and high potency against GT 1 but little activity against GT 2a. Subsequent efforts to optimize LLE and potency led to a 3 log improvement in activity against GT 2a together with a small drop in log *D*. Activity in the low nanomolar range was seen across the broad range of genotypes tested. Representative **20** showed low nanomolar or better inhibitory activity in the 1a, 1b, 2a, 2b, 3a, 4a, and 6a replicon systems.

EXPERIMENTAL SECTION

Chemistry. The purity of the final compounds was determined to be ≥95% by ^{1}H NMR and LCMS; structural asignments were consistent with the spectroscopic data. Solvents were purified and stored according to standard procedures. Flash column chromatography was conducted under medium pressure on silica (ISCO RediSep Rf). HPLC purification was performed on Shimadzu LC instruments, with a 20 min gradient of 0.1% aqueous TFA and 10−97% acetonitrile, at a flow rate of 20 mL/min, using as the stationary phase a Phenomenex SnyderSi4 4 μm Polar RP column, 20 mm × 150 mm, and peak acquisition based on UV detection at 254 nm. NMR spectra were collected on a Varian 300 Inova. Frequencies for nuclei were 400 MHz for ^{1}H and 75 MHz for ^{13}C, using DMSO as solvent unless indicated otherwise. LCMS was performed on a Dionex MSQ, using Phenomenex Synergi Hydro RP 80A column: eluent, water/acetonitrile, formic acid (0.05%); gradient 1% acetonitrile to 100% acetonitrile; run length, 2 or 4 min. Analytical RP-HPLC was performed on Agilent 1100 series with Phenomenex Luna C18 and mobile phase gradual mix of water and acetonitrile containing 0.1% TFA. Monitoring wavelength was 254 nm. High resolution mass spectrometry was performed on an Agilent model 6220 time of flight mass spectrometer with an Agilent 1200 rapid resolution HPLC instrument. Data processing was via Agilent MassHunter B.02 Qualitative Analysis. The lock masses that were used during the run were 118.086 255 and 922.009 798.

(1*S*,3*R*)-3-(5-(8-*tert*-Butyl-4-methyl-6-(2,2,2-trifluoroethylamino)quinolin-2-yl)-1,3,4-oxadiazol-2-ylamino)cyclohexanol (20).

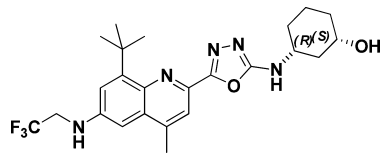

A solution of (1*S*,3*R*)-3-aminocyclohexanol (29 mg, 0.25 mmol) in 1 mL DCM was cooled to 0 °C and treated with *O*-phenyl carbonochloridothioate (447 mg, 0.26 mmol). TEA (77 μL, 0.55 mmol) was added slowly over 15 min with vigorous stirring. After 2 h, the mixture was diluted with 1 mL of 10% citric acid solution and stirred for an additional 5 min. The organic layer was separated (rinsing with additional DCM), dried with sodium sulfate, and concentrated to provide a tan semisolid. This material was taken up in 2 mL of DMF and treated with 8-*tert*-butyl-4-methyl-6-(2,2,2-trifluoroethylamino)quinoline-2-carbohydrazide (67 mg, 0.22 mmol) and TEA (22 mg, 0.22 mmol) and heated to 50 °C for 3 days. The mixture was then cooled to rt and treated with EDCI (110 mg, 0.66 mmol). The mixture was heated to 50 °C for 3 h, then cooled and diluted with EtOAc. The organic solution was washed with water, dried with sodium sulfate, and concentrated to provide an oily brown solid. Purification by silica gel chromatography provided the product

dx.doi.org/10.1021/jm401646w | J. Med. Chem. 2014, 57, 2161−2166

(23 mg, 25% yield) as a white solid. LCMS t_R = 2.38 min; [M + H] = 478.23; ^{19}F NMR δ −70.60 (t, J = 9.7 Hz); ^{1}H NMR (400 MHz, DMSO-d_6) δ 7.92 (s, 1H), 7.83 (d, J = 7.6 Hz, 1H), 7.75 (s, 1H), 7.27 (d, J = 2.5 Hz, 1H), 6.83 (t, J = 6.8 Hz, 1H), 4.65 (d, J = 4.6 Hz, 1H), 4.25−3.88 (m, 2H), 3.41 (d, J = 9.0 Hz, 1H), 2.86 (s, 1H), 2.70 (d, J = 0.7 Hz, 1H), 2.57 (d, J = 1.0 Hz, 3H), 2.18 (d, J = 11.9 Hz, 1H), 1.95 (s, 1H), 1.78 (s, 1H), 1.76−1.60 (m, 2H), 1.59 (s, 9H), 1.35−0.83 (m, 2H). HRMS calcd for $C_{24}H_{30}F_3N_5O_2$, M^+ 477.2352; found, 477.2353.

***N*-((1,3-Dioxolan-2-yl)methyl)-5-(8-*tert*-butyl-4-methyl-6-(2,2,2-trifluoroethoxy)quinolin-2-yl)-1,3,4-oxadiazol-2-amine (4).**

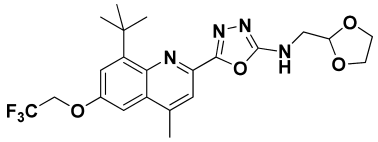

A solution of (1,3-dioxolan-2-yl)methanamine (0.311 mL, 3.02 mmol) and TEA (1.01 mL, 7.24 mmol) in 10 mL DCM was cooled to 0 °C and treated dropwise with thiophosgene (0.28 mL, 3.62 mmol). After being stirred at rt for 2.5 h, the mixture was diluted with Et_2O and washed with water. The organic layer was separated and dried with sodium sulfate before filtering through a plug of silica gel. Concentration provided a faintly yellow oil, which was taken up in 30 mL of DCE, treated with 8-*tert*-butyl-4-methyl-6-(2,2,2-trifluoroethoxy)quinoline-2-carbohydrazide (978 mg, 2.78 mmol), and heated to 65 °C for 2 h. The mixture was then cooled to rt and treated with EDCI (2.02 g, 10.57 mmol) and allowed to stir an additional 16 h. The mixture was finally diluted with 100 mL of EtOAc and washed successively with 10% citric acid and saturated $NaHCO_3$. The organic layer was separated, dried with Na_2SO_4, filtered, and concentrated to provide an off-white solid. Purification by silica gel chromatography with DCM−THF as the mobile phase provided oxadiazole (979 mg, 74% yield) as a white solid. ^{1}H NMR (400 MHz, DMSO-d_6) δ 8.19 (d, J = 6.3 Hz, 1H), 7.91 (s, 1H), 7.40 (s, 1H), 7.32 (s, 1H), 5.04 (t, J = 4.3 Hz, 1H), 4.96 (q, J = 8.9 Hz, 2H), 3.92 (t, J = 6.8 Hz, 2H), 3.80 (t, J = 6.9 Hz, 2H), 3.41−3.35 (m, 2H), 2.69 (s, 3H), 1.61 (s, 9H); ^{19}F NMR (376.1 MHz) δ −72.82, −75.17 (TFA salt); MS $[M + H]^+$ = 467.2; LCMS t_R = 2.58 min. HRMS calcd for $C_{22}H_{25}F_3N_4O_4$, M^+ 466.1828; found, 466.1815.

■ ASSOCIATED CONTENT

Ⓢ Supporting Information

Details for the syntheses and spectroscopic characterization of the compounds in this paper and further assay details. This material is available free of charge via the Internet at http://pubs.acs.org.

■ AUTHOR INFORMATION

Corresponding Author

*Bart Phillips.: Phone: 650-522-5060. E-mail: bart.phillips@gilead.com.

Present Addresses

[†]J.S.: 622 Daisyfield Drive, Livermore, CA 94551.

[‡]C.S.: Accelas Pharmaceutical Inc., No. 9 Weidi Rd., Xianlin University City, Qixia District, Nanjing, China.

Notes

The authors declare the following financial interests: The authors are employees of Gilead Sciences except for C. S. and J. S. who were employed at Gilead Sciences during this research. All authors are shareholders of Gilead Sciences.

■ ACKNOWLEDGMENTS

Special thanks are given to Kathy Brendza for her work obtaining high resolution mass spectral data for the project and to Dharmaraj Samuel and Nikolai Novikov for their work in purifying the NS4B protein.

■ ABBREVIATIONS

AcOH, acetic acid; DCE, dichloroethane; DCM, dichloromethane; DIAD, diisopropyl azodicarboxylate; TEA, triethylamine; EtOAc, ethyl acetate; GT, genotype; Hex, hexanes; HCl, hydrochloric acid; HCV, hepatitis C virus; KHMDS, potassium hexamethyldisilazide; KO-*t*-Bu, potassium *tert*-butoxide; LiHMDS, lithium hexamethyldisilazide; MeCN, acetonitrile; MeOH, methanol; min, minute; NaOAc, sodium acetate; NS, nonstructural; RP, reverse phase; S_NAr, nucleophilic aromatic substitution; WT, wild type

■ REFERENCES

(1) Armstrong, G. L.; Wasley, A.; Simard, E. P.; McQuillan, G. M.; Kuhnert, W. L.; Alter, M. J. The Prevalence of Hepatitis C Virus Infection in the United States, 1999 through 2002. *Ann. Intern. Med.* **2006**, *144*, 705−714.

(2) Poordad, F.; Dieterich, D. Treating Hepatitis C: Current Standard of Care and Emerging Direct-Acting Antiviral Agents. *J. Viral Hepatitis* **2012**, *19*, 449−464.

(3) Nguyene, M. H.; Keeffe, E. B. Prevalence and Treatment of Hepatitis C Virus Genotypes 4, 5, and 6. *Clin. Gastroenterol. Hepatol.* **2005**, *3*, S97−S101.

(4) Nyanguile, O.; Devogelaer, B.; Vijgen, L.; Van den Broeck, W.; Pauwels, F.; Cummings, M. D.; De Bondt, H. L.; An Vos, A. M.; Berke, J. M.; Lenz, O.; Vandercruyssen, G.; Vermeiren, K.; Mostmans, W.; Dehertogh, P.; Delouvroy, F.; Vendeville, S.; VanDyck, K.; Dockx, K.; Cleiren, E.; Raboisson, P.; Simmen, K. A.; Fanning, G. C. 1a/1b Subtype Profiling of Nonnucleoside Polymerase Inhibitors of Hepatitis C Virus. *J. Virol.* **2011**, *84*, 2923−2934.

(5) Halfoni, H. L.; Locarnini, S. Hepatitis C Virus Resistance to Protease Inhibitors. *J. Hepatol.* **2011**, *55*, 192−206.

(6) Melnikova, I. Hepatitis C—Pipeline Update. *Nat. Rev. Drug Discovery* **2011**, *10*, 93−94.

(7) Li, S.; Yu, X.; Guo, Y.; Kong, L. Interaction Networks of Hepatitis C Virus NS4B: Implications for Antiviral Therapy. *Cell. Microbiol.* **2012**, *14*, 994−1002.

(8) Shotwell, J. B.; Baskaran, S.; Chong, P.; Creech, K. L.; Crosby, R. M.; Dickson, H.; Fang, J.; Garrido, D.; Mathis, A.; Maung, J.; Parks, D. J.; Pouliot, J. J.; Price, D. J.; Rai, R.; Seal, J. W., III; Schmitz, U.; Tai, V. W. F.; Thomson, M.; Xie, M.; Xiong, Z. Z.; Peat, A. J. Imidazo[1,2-*a*]pyridines That Directly Interact with Hepatitis C NS4B: Initial Preclinical Characterization. *ACS Med. Chem. Lett.* **2012**, *3*, 565−569.

(9) Roberts, S. D.; Peat, A. J. HCV Replication Inhibitors That Interact with NS4B. In *Successful Strategies for the Discovery of Antiviral Drugs*; Desai, M. C., Meanwell, N. A., Eds.; Royal Society of Chemistry: Cambridge, U.K., 2013; pp 110−145.

(10) Miller, J. F.; Chong, P. Y.; Shotwell, J. B.; Catalano, J. G.; Tai, V. W. F.; Fang, J.; Banka, A. L.; Roberts, C. D.; Youngman, M.; Zhang, H.; Xiong, Z.; Mathis, A.; Pouliot, J. J.; Hamatake, R. K.; Price, D. J.; Seal, J. W.; Stroup, L. L.; Creech, K. L.; Carballo, L. H.; Todd, D.; Spaltenstein, A.; Furst, S.; Hong, Z.; Peat, A. J. Hepatitis C Replication Inhibitors That Target the Viral NS4B Protein. *J. Med. Chem.* [Online early access]. DOI: 10.1021/jm400125h. Published Online: Apr 1, **2013**.

(11) Zhang, X.; Zhang, N.; Chen, G.; Turpoff, A.; Ren, H.; Takasugi, J.; Morrill, C.; Zhu, J.; Li, C.; Lennox, W.; Paget, S.; Liu, Y.; Almstead, N.; Njoroge, F.; Gu, Z.; Komatsu, T.; Clausen, V.; Espiritu, C.; Graci, J.; Colacino, J.; Lahser, F.; Risher, N.; Weetall, M.; Nomeir, A.; Karp, G. M. *Bioorg. Med. Chem. Lett.* **2013**, *23*, 3947−3953.

(12) Zhang, N.; Zhang, X.; Zhu, J.; Turpoff, A.; Chen, G.; Morrill, C.; Huang, S.; Lennox, W.; Kakarla, R.; Liu, R.; Li, C.; Ren, H.; Almstead, N.; Venkatraman, S.; Njoroge, F. G.; Gu, Z.; Clausen, V.; Graci, J.; Jung, S. P.; Zheng, Y.; Colacino, J. M.; Lahser, F.; Sheedy, J.; Mollin, A.; Weetall, M.; Nomeir, A.; Karp, G. M.. Structure−Activity

Relationship (SAR) Optimization of 6-(Indol-2-yl)pyridine-3-sulfonamides: Identification of Potent, Selective, and Orally Bioavailable Small Molecules Targeting Hepatitis C (HCV) NS4B. *J. Med. Chem.* [Online early access]. DOI: 10.1021/jm401621g. Published Online: Nov 22, **2013**.

(13) Kakarla, R.; Liu, J.; Naduthambi, D.; Chang, W.; Mosley, R. T.; Bao, D.; Steuer, H. M. M.; Keilman, M.; Bansal, S.; Lam, A. M.; Seibel, W.; Neilson, S.; Furman, P. A.; Sofia, M. J. Discovery of a Novel Class of Potent HCV NS4B Inhibitors: SAR Studies on Piperazinone Derivatives. *J. Med. Chem.* [Online early access]. DOI: 10.1021/jm4012643. Published Online: January 29, **2014**.